Department of Life Science[1], University of Seoul, Korea; Institute of Pharmacy[2], Ernst Moritz Arndt University, Greifswald, Germany; Department of Biochemistry[3], College of Medicine, Cheju National University, Jeju College of Pharmacy[4], Chung-Nam National University, Taejon, Korea

Apoptosis induction by 4β-acetoxyscirpendiol from *Paecilomyces tenuipes* in human leukaemia cell lines

H. C. Han[1], U. Lindequist[2], J. W. Hyun[3], Y. H. Kim[4], H. S. An[1], D. H. Lee[1], H. W. Kim[1]

Received February 3, 2003, accepted April 30, 2003

Ha Won Kim, Department of Life Science, University of Seoul, Jeonnong-Dong, Seoul 130–743, Korea
hwkim@uos.ac.kr

Pharmazie 59: 42–49 (2004)

The carpophores of *Paecilomyces tenuipes* are known in the Orient for their strong antitumor activity. In continuation of our study on acetoxyscirpendiol (ASD, 4β-acetoxyscirpene-3α,15-diol) as a cytotoxic component from this fungus, we report particularly on the mode of action of ASD in inducing apoptosis in human MOLT-4, THP-1 and Jurkat T cell leukaemia *in vitro*. The antiproliferative effects of ASD seem attributable to its induction of apoptosis in the cells, as it blocked the cell cycle, induced hypodiploidity and bound annexin V and also cleaved poly-(ADP-ribose) polymerase (PARP) in these cell lines. The 50% inhibitory concentrations (IC_{50}) of ASD on MOLT-4, THP-1 and Jurkat T cells were found to be 60, 85 and 60 ng/ml, respectively. ASD arrested the cell cycle at the G_1/S transition and showed hypodiploidity due to the accumulation of sub-G_0 population. Annexin V binding was increased in the presence of ASD in the MOLT-4 cell line in a time-dependent manner. ASD and three of its derivatives also induced cleavage of PARP in both MOLT-4 and Jurkat T cell lines. From these data, it is suggested that ASD exerts its cytotoxic activity by inducing apoptosis in leukaemia cell lines *in vitro*.

1. Introduction

The fungus *Paecilomyces tenuipes* is a caterpillar fungus, like *Cordyceps*. Chinese caterpillar fungi are one of the most valuable tonic foods and herbal medicines in China and in the neighbouring countries. These entomogenous mycelia grow in and derive nutrients from their host insect in the autumn and fruiting bodies of the fungus protrude from the body in the following summer (Halpern 1999). According to traditional Chinese medicine, these fungi have been used as remedies for cancer, tuberculosis, asthma, allergic diseases and endocrine disorders (Jones 1997 for review; Zhu et al. 1998a; Zhu et al. 1998b). Despite its extensive medicinal use, little is known about the biologically active compounds of *P. tenuipes* due to its scarce supply. This fungus, however, is now available in large quantity thanks to the success of artificial cultivation. In a previous paper, we reported the isolation of a cytotoxic compound, acetoxyscirpendiol (ASD, 4β-acetoxyscirpene-3α,15-diol) together with ergosterol peroxide from the fruiting bodies of *P. tenuipes* (Nam et al. 2001).

ASD belongs structurally to the trichothecenes which are produced by various species of imperfect fungi. Trichothecenes possess cytotoxic (Abbas et al. 2002), antiviral (Tani et al. 1995) and hemolytic activities (Segal et al. 1983). The cytotoxic activity of trichothecenes in mammalian cells results from inhibition of protein and DNA synthesis. Some trichothecenes inhibit the initiation step in protein synthesis on polysomes and others inhibit the elongation/termination step in protein synthesis (Cole and Cox 1981). All common trichothecenes have a 9,10 double bond and a 12,13 epoxide group. ASD has a monoacetoxy group at the C-4 position.

Trichothecenes have been reported to induce apoptosis *in vivo* (Zhou et al. 2000) and *in vitro* (Yang et al. 2000). Apoptosis or programmed cell death is a regulated physiological phenomenon leading to cell death characterized by cell shrinkage, membrane blebbing, activation of caspases, release of cytochrome c from mitochondria and DNA fragmentation (Ashkenazi and Dixit, 1998). PARP is a nuclear DNA binding protein of 113 kDa that is constitutively expressed in eucaryotes (Alvarez-Gonzalez et al. 1999). At lower levels of DNA damage, PARP activity protects against apoptosis, because PARP inhibits the pro-apoptotic endonuclease through poly(ADP) ribosylation (Bernstein et al. 2002). Intact 113 kDa PARP is cleaved into 89 and 24 kDa fragments by caspase-3 during early apoptosis (Boulares et al. 1999). Some trichothecenes induce apoptosis by activating c-Jun N-terminal kinase and p38 mitogen-activated protein kinase (Shifrin and Anderson 1999). Other trichothecenes also induce apoptosis by activating mitogen-activated protein kinases (MAPKs) such as extracellular signal-regulated protein kinase (ERK), p38 MAPK, and stress-activated protein kinase/c-Jun N-terminal kinase (SAPK/JNK) in myeloid cells (Yang et al. 2000). Recently, it was reported that ASD isolated from the fruiting bodies of *Isaria japonica* induces apoptosis by activating caspase-3 in human leukemia HL-60 cells (Oh et al. 2001).

In this study, we characterized the cytotoxic activities of ASD focusing on induction of apoptosis for example by hypodiploidity, binding of annexin V and cleavage of poly-(ADP-ribose) polymerase (PARP). In addition to ASD, we found that derivatives of ASD also induced cleavage of PARP in a time-dependent manner. Cleavage of PARP was much more sensitive in Jurkat T cells than in MOLT-4 cells in spite of their similar IC_{50} values in those cell lines.

2. Investigations and results

2.1. Inhibition of cell growth by ASD

The effect of ASD on the viability of MOLT-4 and THP-1 cells was assessed using the MTT test at day 3 of the cultures and 50% growth inhibitory concentration (IC_{50}) values were determined. When the cells were treated with various concentrations of ASD it significantly reduced MOLT-4 and THP-1 cell viabilities in a dose-dependent manner. IC_{50} values were determined to be 60 and 85 ng/ml, respectively (Fig. 1A). In a separate experiment, the IC_{50} of ASD was 60 ng/ml in Jurkat T cells. In order to monitor the time-course of the cell viability, the cell numbers were counted every 12 h for 72 h. The non-treated cells began to proliferate exponentially 24 h after the beginning of cultivation. However, both cell lines treated with 200 ng/ml ASD failed to proliferate (Fig. 2B).

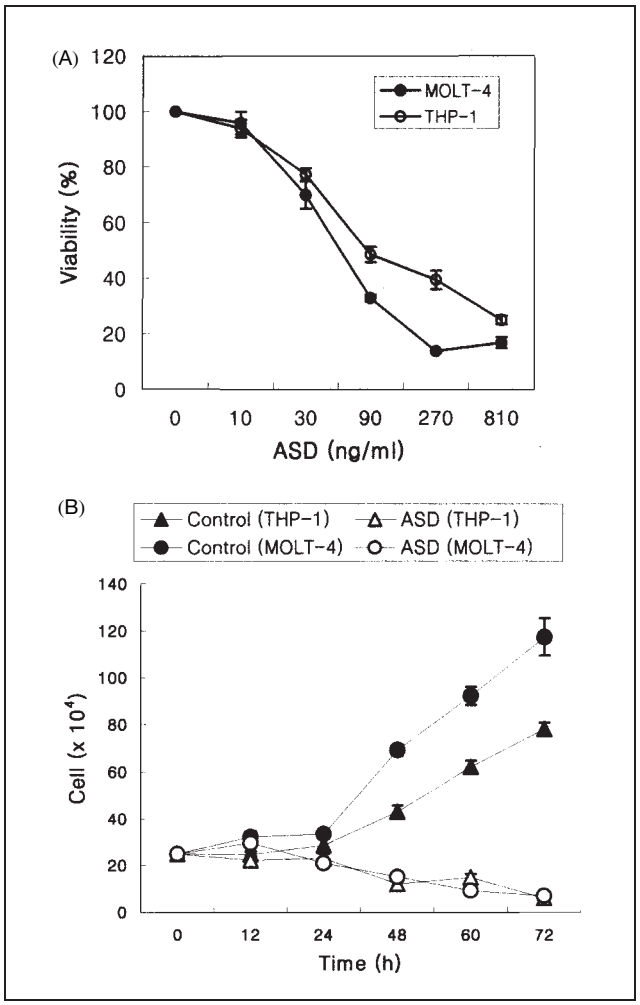

Fig. 1: Concentration and time-course effects of acetoxyscirpendiol (ASD) on cell viability of MOLT-4 (●) and THP-1 (○) cells. (A) Cells were cultured with ASD at final concentrations of 0, 10, 30, 90, 270 and 810 ng/ml in 96-well plates. The viability of the cells was determined at 72 h by MTT assay. (B) Cells were incubated with 200 ng/ml of ASD in 96-well plates and viable cells were counted by trypan blue dye exclusion method. Data are expressed as mean ± SD of three wells. Error bars represent SD of three duplicates

2.2. Arrest of cell cycle

The effect of ASD on cell cycle progression of MOLT-4 cells was determined. Cell cycle status was assessed by FACSCalibur flow cytometer (Becton Dickinson Co., USA), staining nuclei with PI. The cell cycle patterns showed a raised proportion of events in the G_0/G_1 and a decreased proportion of events in the G2/M phase when compared with time-matched, vehicle-treated controls during 72 h of culture. Treatment with 60 ng/ml ASD on logarithmically growing MOLT-4 cells resulted in 71, 67, 77 and 72% of G_0/G_1 phase cell populations at 1, 48, 60 and 72 h compared with control values of 69, 58, 59 and 59%, respectively (Fig. 2). The cell populations of the G2/M phase of the ASD treated group were 6.3, 0, 0 and 0% at 1, 48, 60 and 72 h, while control values were 6.9, 8.4, 13.7 and 8.1%, respectively. Interestingly, the cell population of the sub-G1 phase was greatly increased compared to that of the control. In terms of cell cycle distribution, THP-1 cells were similar to MOLT-4 (data not shown). These results are indicative of blocking the G_1/S transition by ASD.

2.3. Induction of hypodiploidity

The increased population of the sub-G1 phase in Fig. 2 might indicate blebbing of the cells by treatment with ASD. We thus analyzed the population of sub-G1 phase over time during the 72 h after treating MOLT-4 and THP-1 cells with 200 ng/ml of ASD. Induction of cell death by apoptosis begins with blebbing of the cells resulting in a hypodiploid apoptotic body. The population of the sub-G1 phase calculated by fluorescence-activated cell sorting (FACS) analysis was considered as the hypodiploid cell population. Cells were incubated with 200 ng/ml ASD for 0, 12, 24, 36, 48, 60 and 72 h. The proportion of hypodiploidity in the control cell population was between 1% and 3%. In ASD treated cells, however, hypodiploid cell populations in MOLT-4 and THP-1 cells were 70.2% and 40.6%, respectively, for an incubation time of 72 h (Fig. 3). ASD increased the hypodiploid cell population in a time-dependent manner. The sensitivity against ASD was higher in the MOLT-4 than in the THP-1 cell line. These results imply that the increased hypodiploid cell population with ASD treatment may be due to the formation of apoptotic bodies rather than necrotic cell death.

2.4. Annexin V binding analysis

Considering that ASD blocked the cell cycle and increased the population of hypodiploid cells, we monitored membrane phosphatidyl serine (PS) translocation by analyzing annexin V-FITC bound cell population by a flow cytometric method. During the course of apoptosis in cells, annexin V tends to bind to PS translocated from the inner plasma membrane to the outer cell surface (Wang et al. 2001). When MOLT-4 cells were treated with 200 ng/ml of ASD, binding between annexin V-FITC and PS appeared to increase in a time-dependent manner (Fig. 4). The populations of annexin V bound cells among at least 8,000 events collected for analysis were 0.6%, 7.1%, 9.0% and 41.5% at 0, 12, 24 and 48 h incubation,

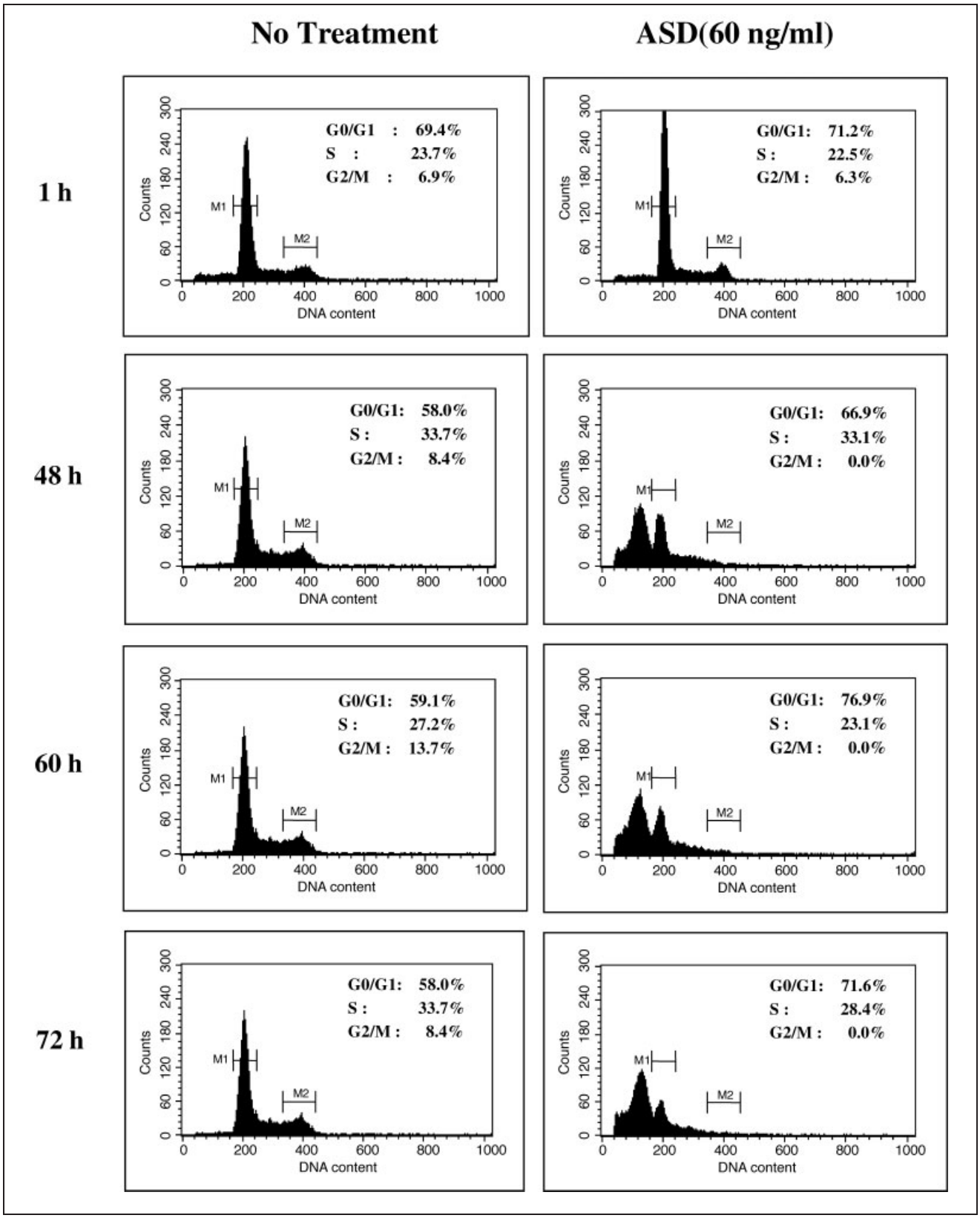

Fig. 2: Effect of ASD on cell cycle phase distribution in MOLT-4 cell. Cells (1×10^6) were cultured in the presence or absence of 60 ng/ml of ASD for 1, 48, 60 and 72 h. Cells were harvested and stained with propidium iodide for cell cycle analysis. Cell cycle status was assessed by FACSCalibur flow cytometer. Data shown represent pattern values of three independent experiments

respectively. The mean fluorescence intensity of the annexin V bound cell population was 14, 20, 31 and 263 at incubation times of 0, 12, 24 and 48 h, respectively. These data strongly indicate that ASD induced PS translocation in the cell membrane.

2.5. Induction of PARP cleavage

One of the typical phenomena of apoptosis is fragmentation of DNA which could be prevented by activation of PARP. Apoptotic signals induce cleavage of 113 kDa

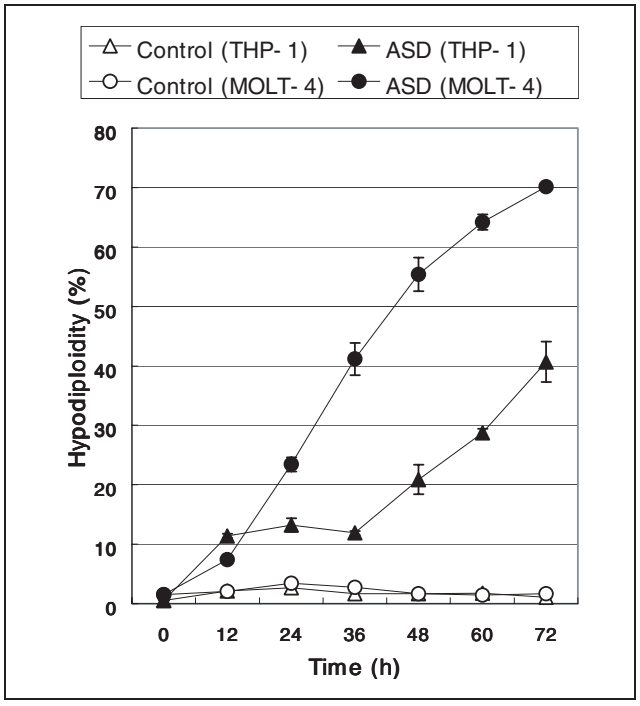

Fig. 3: Time course experiment on hypodiploidity of DNA induced by ASD in MOLT-4 and THP-1 cells. Cells (1×10^6) were treated with 200 ng/ml ASD up to the indicated time points and DNA was analyzed by flow cytometry after staining with PI. Data are expressed as mean ± SD of three wells

PARP into 89 kDa and 24 kDa. We measured the extent of cleavage of PARP following the treatment of MOLT-4 cells with 500 ng/ml ASD for 0, 24 and 48 h. When we compared the band intensity ratio of 113 kDa intact PARP and 89 kDa PARP fragment, ASD induced PARP cleavage of 7% and 11% at 24 and 48 h incubation, respectively (Fig. 5A). We then compared the activity of ASD on the cleavage of PARP in MOLT-4 cells with that of its derivatives. Unexpectedly, the activity of the derivatives 1-AS, 2-AS and 3-AS, mono-, di- and tri-acetoxyscirpenol, on the cleavage of PARP was shown to be much stronger than that of ASD. The PARP cleavage activity of 1-AS, 2-AS and 3-AS at 24 h incubation was 36, 29 and 41% and that at 48 h incubation was 62, 80 and 82%, respectively. All the derivatives showed time-dependent PARP cleavage activities (Fig. 5B). As ASD showed a very weak PARP cleavage activity in the MOLT-4 cell line in Fig. 5A, we compared its PARP cleavage activity in Jurkat T cells with that of its derivatives. The non-treated control group was not cleaved while staurosporine (93 ng/ml) as a positive control induced 34% cleavage of PARP. When Jurkat T cells were treated with 1-AS (50 ng/ml), 2-AS (50 ng/ml), 3-AS (50 ng/ml) and ASD (100 ng/ml) for 12 h, PARP cleavage ratios were 32, 81, 48, and 40%, respectively (Fig. 5C). From these data, ASD induced PARP cleavage much more strongly in Jurkat T cells than in MOLT-4 cells even at a lower concentration and for a shorter time.

3. Discussion

In this study, we demonstrated evidence for apoptosis induced by the compound ASD whose structure elucidation and purification from the carpophores of *P. tenuipes* was reported in our previous study (Nam et al. 2001). When treated with ASD, the two cancer cell lines, MOLT-4 and THP-1, exhibited typical apoptotic phenomena such as blocking of the cell cycle, induction of hypodiploidity and annexin V binding. ASD induced very strong cleavage of PARP in Jurkat T cells although PARP cleaving activity appeared relatively weak in MOLT-4 cells.

ASD belongs to the family of trichothecenes which are structurally related sesquiterpenoid metabolites in fungi imperfecti such as *Fusarium, Cordyceps* and *Paecilomyces* species. Trichothecenes induce apoptosis not only by activating extracellular signal-regulated protein kinase (ERK) in myeloid cell lines (Yang et al. 2000), but also by activating c-Jun N-terminal kinase (JNK) and p38 MAPK (Shifrin and Anderson 1999). Trichothecenes block protein biosynthesis through inhibiting peptidyltransferase reaction by binding to the 60 S ribosomal subunit in eukaryotic cells (Middlebrook and Leatherman 1989). Blocking of protein synthesis is known to induce apoptosis in some cell lines (Coxon et al. 1998; Geier et al. 1996). However, our present results show that PARP cleavage could be one of the causes for apoptosis in leukaemia cell lines by the trichothecenes.

At various concentrations, ASD strongly inhibited cell growth in MOLT-4, THP-1 and Jurkat T cells. The retarded cell growth coincided with the arrested cell cycle, hypodiploidity and DNA fragmentation, which are characteristic of apoptosis. The DNA cell cycle analysis, quantified by flow cytometry, showed that an IC_{50} concentration of ASD arrested the G_1/S phase of the cell cycle with a concomitant decrease in the cell percentage of the G2/M phases. However, the cell population at the S phase was not changed until 48 h incubation. These results provide strong support for ASD's apoptotic potential considering many apoptosis inducing agents arrest the cell cycle at G_1/S (Katdare et al. 2002; Wang et al. 2002; Chinni and Sarkar, 2002) or G2/M phase (Ferry-Dumazet et al. 2002) depending on their properties in the cell cycle to remove irrepairably damaged cells.

In our previous studies on cell cycle related-gene expression, ASD increased expression of mRNA and protein levels of both cyclin C and mitotic arrest deficient like-1 (Mad-1) in the human breast cancer MCF-7 cell line (Chung et al. 2003). Cyclin C belongs to the cyclin family of proteins and there is little evidence for the role of cyclin C in cell cycle regulation. The only known function of cyclin C is in transcriptional machinery for RNA polymerase II (Boyer et al. 1999) and no direct support for a role in the promotion of cell cycle progression has been observed thus far (Liu et al. 1998). Rather, degradation of cyclins is required for cell-cycle progression. Over − expression of Mad-1 also shows anti-proliferation and blockage of the cell cycle at the G_1/S phase in a melanoma cell line (Ohta et al. 2002). Our present finding of cell cycle blockage by ASD concurs with the previous report on the increase of both cyclin C and Mad-1 expression.

ASD caused hypodiploidity due to the formation of apoptotic bodies. ASD also led to annexin V binding to PS translocated from the inner plasma membrane to the outer cell surface in the MOLT-4 leukemia cells. In order to analyze further the molecular mechanism by which ASD causes cell cycle arrest, we evaluated PARP cleavage in MOLT-4 cells. ASD cleaved PARP weakly in the MOLT-4 cell line. We wanted to know whether derivatives of ASD could induce PARP cleavage in the same cell line. The scirpentriol family has hydroxyl groups at the 3, 4 and 15 positions. In the scirpenol family all the hydroxyl groups could be acetylated. As ASD has one acetoxyl group at position 4, we used 1-AS which has an acetoxyl group at

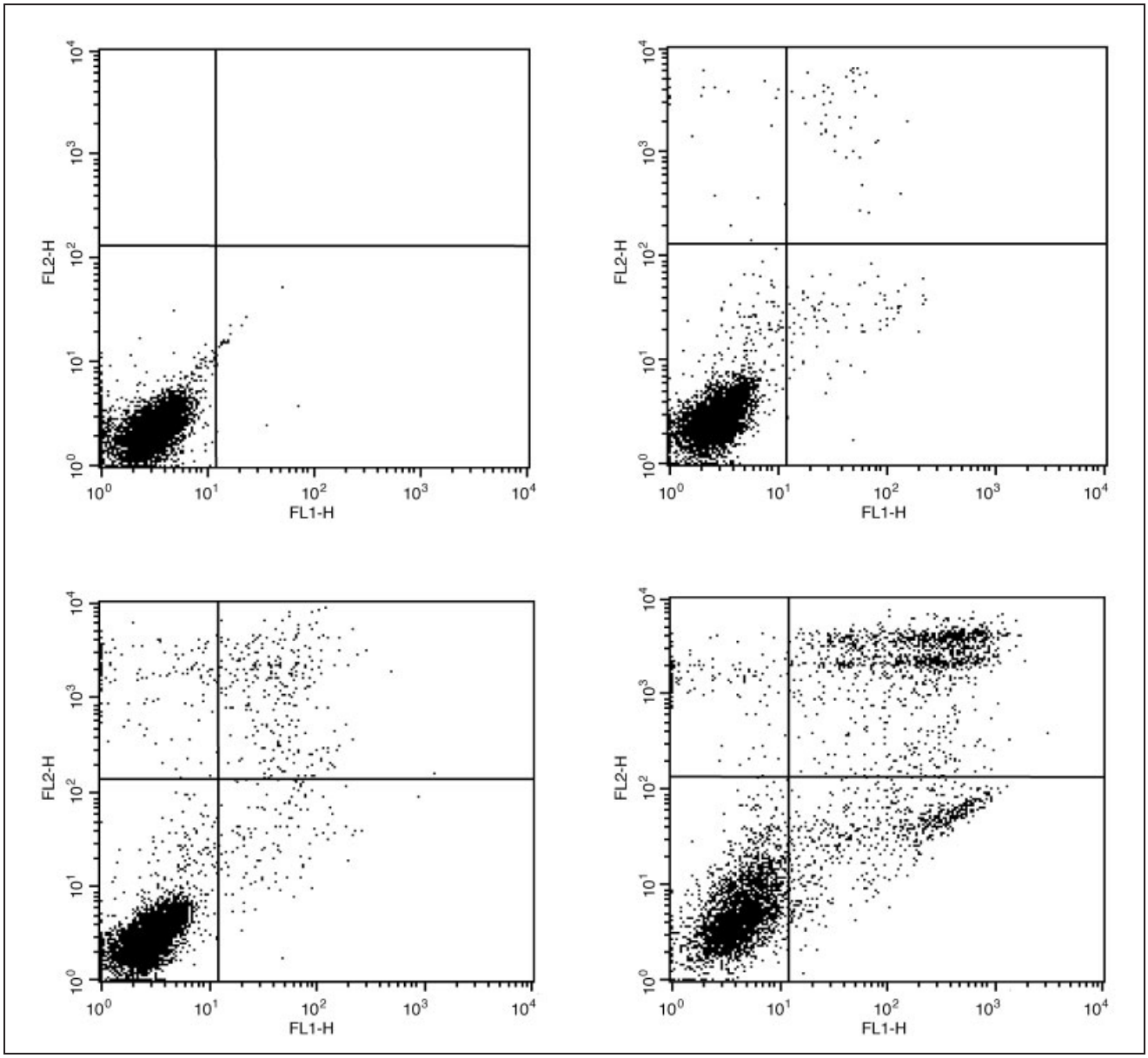

Fig. 4: Binding of FITC-annexin V on ASD treated MOLT-4 cells. Cells (1×10^6) were treated with 200 ng/ml of ASD for 0, 12, 24 and 48 h. PI and FITC-annexin V co-stained cells were analyzed at 0 (A), 12 (B), 24 (C) and 48 h (D) by flow cytometry

position 15, 2-AS which has two acetoxyl groups at positions 4 and 15, and 3-AS which has three acetoxyl groups at positions 3, 4 and 15. All the derivatives tested exerted much stronger cleavage of PARP than that of ASD in MOLT-4 cells in a time dependent manner. All the derivatives showed similar cleavage activities in MOLT-4 cells after 24 h exposure. However, difference in cleavage was evident among the derivatives for 48 h incubation.

4,15-Diacetoxyscirpenol is known as the most toxic among the acetylated scirpenols (Richardson and Hamilton 1990). In our study, 2-AS and 3-AS showed much stronger activity than ASD and 1-AS, indicating that acetoxyl groups at both positions 4 and 15 seem essential to sustain strong activity in PARP cleavage. We then compared PARP cleavage in another T cell leukaemia, Jurkat T cell. Interestingly, in spite of the similar IC_{50} values of 60 ng/ml in MOLT-4 and Jurkat T cells, ASD induced much stronger PARP cleavage activity in Jurkat T cells than in MOLT-4 cells in a time-dependent manner. We could induce PARP cleavage with much lower concentration of all the reagents and a much shorter incubation in Jurkat T cells. Thus, 12 h exposure with ASD, 1-AS, 2-AS and 3-AS showed strong PARP cleavages in Jurkat T cells. Among the derivatives, 2-AS showed the strongest PARP cleavage activity in Jurkat T cells. This toxicity concurs with the brine shrimp lethality test where 2-AS showed the strongest cytotoxicity (Richardson and Hamilton 1990).

Apoptotic cell death is often mediated by a caspase cascade. Activated caspase-3 cleaves 113 kDa intact PARP into an 89 kDa fragment which has no protective activity against apoptosis. PARP synthesizes poly(ADP-ribose) from NAD in response to DNA strand breakage and plays an important role in DNA base excision repair (Bahtia and Smulson 1990). Therefore, cleaved PARP could not repair broken DNA strands. Our finding of PARP cleavage by ASD could be supported by a report of caspase-3 activation by ASD (Oh et al. 2001). Activation of caspase-3 by ASD could induce cleavage of PARP in MOLT-4 and Jurkat T cells.

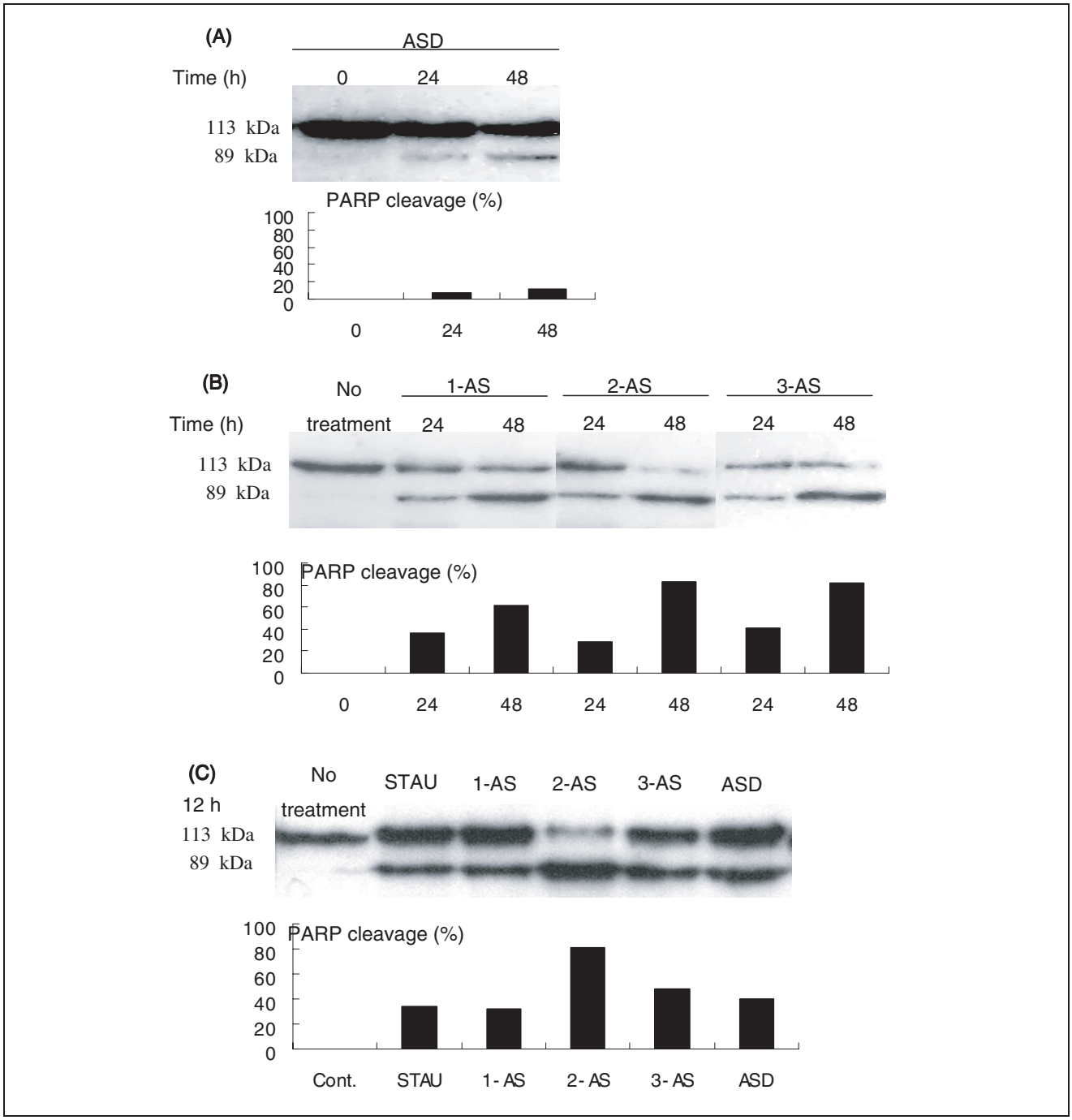

Fig. 5: PARP cleavage induced by ASD in MOLT-4 cells and Jurkat T cells. MOLT-4 cells were incubated with ASD (A) and its derevatives (B) of 1-AS, 2-AS and 3-AS at the concentration of 500 ng/ml for the indicated time points. The cell lysates were subjected to immunoblot analysis with antibodies against PARP. Jurkat T cells (C) were treated with ASD (100 ng/ml), sturosporine (93 ng/ml), 1-AS (50 ng/ml), 2-AS (50 ng/ml) or 3-AS (50 ng/ml) for 12 h. The positions of full-length (113 kDa) PARP and of the proteolytic fragment (89 kDa) are indicated. Quantifications of PARP cleavage were performed with Kodak KDS1D image analyzer. The data shown are typical results for three independent experiments. Abbreviations: ASD, 4β-acetoxyscirpendiol; 1-AS, 15-aceyoxyscirpenol; 2-AS, 4,15-diacetoxyscirpenol; 3-AS, 3α-acetyldiacetoxyscirpenol; STAU, staurosporine

This study provides evidence that ASD induced various changes typical of apoptosis as well as reduced cell viability in the cancer cell lines. Moreover, ASD and its three derivatives induced PARP cleavage in MOLT-4 and Jurkat T cells. The acetoxyscirpenol mycotoxin family showed much stronger and sensitive cleavage of PARP in Jurkat T cells than in MOLT-4 T lymphoblastoma. Taken together, the cytotoxic activity of ASD seems to be a result of apoptosis in the cell lines tested. These results may provide important information for understanding the possible mechanism whereby the acetoxyscirpenol family induces apoptosis in leukaemia cell lines.

4. Experimental

4.1. Cells and reagents

Cell lines used in this study were obtained from the American Type Culture Collection (Rockville, USA) including human MOLT-4 (ATCC CRL-1582) acute T lymphoblastoma, human THP-1 (ATCC TIB-202) acute monocytic leukaemia and human Jurkat T (ATCC TIB-152) leukaemia. The cells were maintained at 37 °C in a humidified 5% CO_2 incubator. The cells were cultured in RPMI1640 medium supplemented with 10% heat-inactivated fetal calf serum, 100 unit/ml penicillin and 100 μg/ml streptomycin. Exponentially growing cells were used throughout the study. Acetoxyscirpendiol (ASD, $C_{17}H_{24}O_6$, 4β-acetoxyscirpene-3α,15-diol) was isolated and recrystalized from the carpophores of *P. tenuipes* as reported previously (Nam et al. 2001). The purity of the ASD was more than 98%

determined by TLC. 15-Acetoxyscirpendiol (1-AS, $C_{17}H_{24}O_6$, more than 99% purity by TLC), diacetoxyscirpenol (2-AS, $C_{19}H_{26}O_7$, more than 99% purity by TLC), 3α-acetyldiacetoxyscirpenol (3-AS, $C_{21}H_{28}O_8$, more than 99% purity by TLC), 3-[4,5-dimethylthiazol-2-yl]-2,5-diphenyltetrazolium bromide (MTT), propidium iodide (PI), dimethyl sulfoxide (DMSO), Bradford reagent, staurosporine, pepstatin A, leupeptin, PMSF, aprotinin and RNAse A were purchased from Sigma Chemical Co. (St. Louis, Mo, USA). Mouse anti-PARP monoclonal antibody and fluorescein isothiocyanate-annexin V conjugate were from BD Biosciences Pharmingen (San Diego, USA). HRP-conjugated goat anti-mouse IgG antibody was from Southern Biotechnology Associates, Inc. (Birmingham, USA). Nitrocellulose transfer membrane was from Schleicher & Schuell GmbH (Dassel, Germany). Enhanced chemiluminescence (ECL) detection kit was from Amersham Pharmacia Biotech (San Francisco, USA).

4.2. Cell viability

Cell viability was determined by the trypan blue exclusion assay counting with a haemacytometer and by MTT. For the MTT, cells were cultured in 96-well culture plates in the presence or absence of ASD dissolved in DMSO and diluted with culture medium. The optimum number of cells to be plated into flat-bottomed 96-well plates was determined by preliminary studies such that cells were in the exponential growth phase at the end of the 3-day incubation. The maximum concentration of the DMSO was less than 1% (v/v) in all the cultures. The cells (1×10^5 cells/well) in 96-well microtiter plates were incubated at 37 °C in a humidified atmosphere of 5% CO_2 for 4 days. After incubation, 0.1 mg (20 µl of a 5 mg/ml solution) of MTT was added to each well and then incubated further for 4 h. The plates were then centrifuged at 1000 rpm for 5 min at room temperature and the medium was then aspirated carefully so as not to disturb the formazan crystals at the bottom of the wells. One hundred microliters of 0.04 N HCl in isopropanol were added to each well to solubilize the formazan crystals. The plates were read immediately at 540 nm on a Benchmark microplate reader (Bio-Rad, USA). All experiments were performed three times and the mean absorbance values were determined.

4.3. Cell cycle and hypodiploidity analyses

FACS analysis of DNA content was performed to assess the cell cycle phase distribution. One million cells per test were harvested at various times and fixed at 4 °C with 1 ml of 80% ethanol for 1 h. Cells were washed twice with PBS buffer and incubated in the dark with 100 µg/ml PI and 100 µg/ml RNAse A at 37 °C for 30 min. Fluorescence emitted from the PI-DNA complex was quantitated after laser excitation of the fluorescent dye using a FACSCalibur flow cytometer. The Cell Quest and Mod-Fit computer programs were used to generate histograms, which were used to determine the cell cycle phase distribution. Hypodiploidity was calculated from the percentage of subdiploid quantities of DNA.

4.4. Annexin V binding analysis

FACS analyses of apoptosis were performed by co-staining with PI and FITC-annexin V conjugate. PI was used to identify broken DNA as a feature of late apoptosis, and annexin V was used to assess aberrant PS exposure (Wang et al. 2001). Staining was performed according to the manufacturer's directions. Briefly, cells (1×10^6) were treated with 200 ng/ml ASD at the final concentration and incubated at 37 °C for 0, 12, 24 and 48 h. Cells were washed twice with cold PBS and resuspended in binding buffer (0.01 M HEPES, pH 7.4; 0.14 M NaCl; 2.5 mM $CaCl_2$) to a concentration of 1×10^6 cells/ml. Each 100 µl of the cell solution was transferred to a 5 ml culture tube and FITC-annexin V and PI were added according to the instructions. Shortly after a 15-min-incubation at room temperature in the dark, each tube was analyzed by a flow cytometer.

4.5. PARP cleavage analysis by Western blot

PARP cleavage was assayed following ASD treatment on MOLT-4 cells and Jurkat T cells. MOLT-4 cells were incubated with ASD or its derivatives, 1-AS, 2-AS and 3-AS, at a concentration of 500 ng/ml for 0, 24 and 48 h. For Jurkat T cells, cells were treated with ASD (100 ng/ml), staurosporine (93 ng/ml), 1-AS (50 ng/ml), 2-AS (50 ng/ml) or 3-AS (50 ng/ml) for 12 h. Cells were then harvested and washed twice with cold PBS (pH 7.4). They were lysed for 30 min on ice in lysis buffer (50 mM Tris-Cl, pH 8.0, 150 mM NaCl, 0.02% sodium azide, 0.5% sodium deoxycholate, 0.1% SDS, 1% NP-40, 2 µg/ml pepstatin A, 2 µg leupeptin, 104.4 µg/ml PMSF, 2 µg/ml aprotinin), followed by high speed centrifugation at 12,000 × g. Protein concentration was determined according to the Bradford method. Twenty to thirty µg protein of the lysate was electrophoresed per lane on 8 or 12% SDS-PAGE and electroblotted onto nitrocellulose membrane. After blocking for 2 h in TBS-T buffer (10 mM Tris-Cl, pH 7.6, 150 mM NaCl) supplemented with 5% non-fat dry milk and 0.1% Tween 20, the membrane was incubated with mouse anti-PARP monoclonal antibody (1 : 500 dilution) and HRP-conjugated goat anti-mouse IgG antibody (1 : 5,000 dilution). The bands of full-length (113 kDa) PARP and of the proteolytic fragment (89 kDa) were detected by ECL detection reagents and then the membrane was exposed on to X-ray film in the darkroom (Johnson and Boise 1999). The intensity of PARP cleavage bands was analyzed with Kodak KDS1D and Cyclone image analyzers.

4.6. Statistical analysis

Data for cell cycle phase and hypodiploidity were analyzed by Cell Quest and Mod-Fit software. All data were expressed as mean ± standard deviation (SD) of the sample examined.

Acknowledgements: This work was supported by a Korea Research Foundation Grant (KRF-2000–015-DP0414). The authors wish to express thanks for the support. The instrumental analysis by FACS and Cyclone Image Processor was made possible by the Modern Instrument Support Program of the University of Seoul. The authors would also like to express thanks to the Entomopathogenic Fungal Culture Collection of Kangwon National University for their supply and identification of *Paecilomyces tenuipes.*

References

Abbas HK, Johnson BB, Shier WT, Tak H, Jarvis BB, Boyette CD (2002) Phytotoxicity and mammalian cytotoxicity of macrocyclic trichothecene mycotoxins from *Myrothecium verrucaria*. Phytochem 59: 309–313.

Alvarez-Gonzalez R, Spring H, Miller M, Birkle A (1999) Selective loss of poly(ADP-ribose) and the 85-kDa fragment of poly(ADP-ribose) polymerase in nucleoli during alkylation-induced apoptosis of HeLa cells. J Biol Chem 274: 32122–32126.

Ashkenazi A, Dixit VM (1998) Death receptors: signaling and modulation. Science 281: 1305–1308.

Bernstein C, Bernstein H, Payne CM, Garewal H (2002) DNA repair/pro-apoptotic dual-role proteins in five major DNA repair pathways: fail-safe protection against carcinogenesis. Mutat Res 511: 145–178.

Bhatia K, Smulson ME (1990) Poly (ADP-ribose) polymerase gene: direct or indirect involvement in DNA repair and malignancy? Prog Clin Biol Res 340A: 233–240.

Boulares AH, Yakovlev AG, Ivanova V, Stoica BA, Wang G, Lyer S, Smulson M (1999) Role of poly(ADP-ribose) polymerase (PARP) cleavage in apoptosis. Caspase 3-resistant PARP mutant increases rates of apoptosis in transfected cells. J Biol Chem 274: 22932–22940.

Boyer TG, Martin MED, Lees E, Ricciardi RP, Berk AJ (1999) Mammalian Srb/Mediator complex is targeted by adenovirus E1A protein. Nature 399: 276–279.

Chinni SR, Sarkar FH (2002) Akt inactivation is a key event in indole-3-carbinol-induced apoptosis in PC-3 cells. Clin Cancer Res 8: 1228–1236.

Chung EJ, Choi K, Kim HW, Lee DH (2003) Analysis of cell cycle gene expression responding to acetoxyscirpendiol isolated from Paecilomyces tenuipes. Biol Pharm Bull 26: 32–36.

Cole RJ, Cox RH (1981) Handbook of toxic fungal metabolites, Academic Press, New York, p. 152–263.

Coxon FP, Benford HL, Russell RG, Rogers MJ (1998) Protein synthesis is required for caspase activation and induction of apoptosis by bisphosphonate drugs. Mol Pharmacol 54: 631–638.

Ferry-Dumazet H, Garnier O, Mamani-Matsuda M, Vercauteren J, Belloc F, Billiard C, Dupouy M, Thiolat D, Kolb JP, Marit G, Reiffers J, Mossalayi MD (2002) Resveratrol inhibits the growth and induces the apoptosis of both normal and leukemic hematopoietic cells. Carcinogenesis 23: 1327–1333.

Geier A, Bar-Shalom I, Beery R, Haimsohn M, Hemi R, Malik Z, Lunenfeld B, Karasik A (1996) Induction of apoptosis in MDA-231 cells by protein synthesis inhibitors is suppressed by multiple agents. Cancer Invest 14: 435–444.

Halpern GM (1999) Cordyceps, China's healing mushroom. Avery Publishing Group, New York, p. 7–14.

Johnson BW, Boise LH (1999) Bcl-2 and caspase inhibition cooperate to inhibit tumor necrosis factor-alpha-induced cell death in a Bcl-2 cleavage-independent fashion. J Biol Chem 274: 18552–18558.

Jones K (1997) Cordyceps, tonic food of ancient China. Sylvan Press, Seattle, p. 13–16.

Katdare M, Osborne M, Telang NT (2002) Soy isoflavone genistein modulates cell cycle progression and induces apoptosis in HER-2/neu oncogene expressing human breast epithelial cells. Int J Oncol 21: 809–815.

Liu ZJ, Ueda T, Miyazaki T, Tanaka N, Mine S, Tanaka Y, Taniguchi T, Yamamura H, Minami Y (1998) A critical role for cyclin C in promotion of the hematopoietic cell cycle by cooperation with c-Myc. Mol Cell Biol 18: 3445–3454.

Middlebrook JL, Leatherman DL (1989) Binding of T-2 toxin to eukaryotic cell ribosomes. Biochem Pharmacol 38: 3103–3110.

Nam KS, Jo YS, Kim YH, Hyun JW, Kim HW (2001) Cytotoxic activities of acetoxyscirpenediol and ergosterol peroxide from *Paecilomyces tenuipes*. Life Sci 69: 229–237.

Oh GS, Hong KH, Oh H, Pae HO, Kim IK, Kim NY, Kwon TO, Shin MK, Chung HT (2001) 4-Acetyl-12,13-epoxyl-9-trichothecene-3,15-diol isolated from the fruiting bodies of *Isaria japonica* Yasuda induces apoptosis of human leukemia cells (HL-60). Biol Pharm Bull 24: 785–789.

Ohta Y, Hamada Y, Saitoh N, Katsuoka K (2002) Effect of the transcriptional repressor Mad1 on proliferation of human melanoma cells. Exp Dermatol 11: 439–447.

Richardson KE, Hamilton PB (1990) Comparative toxicity of scirpentriol and its acetylated derivatives. Poultry Sci 69: 397–402.

Segal R, Milo-Goldzweig I, Joffe AZ, Yagen B (1983) Trichothecene-induced hemolysis. I. The hemolytic activity of T-2 toxin. Toxicol Appl Pharmacol 70: 343–349.

Shifrin VI, Anderson P (1999) Trichothecene mycotoxins trigger a ribotoxic stress response that activates c-Jun N-terminal kinase and p38 mitogen-activated protein kinase and induces apoptosis. J Biol Chem 274: 13985–13992.

Tani N, Dohi Y, Onji Y, Yonemasu K (1995) Antiviral activity of trichothecene mycotoxins (deoxynivalenol, fusarenon-X, and nivalenol) against herpes simplex virus types 1 and 2. Microbiol Immunol 39: 635–637.

Wang Z, Jiang C, Lu J (2002) Induction of caspase-mediated apoptosis and cell-cycle G1 arrest by selenium metabolite methylselenol. Mol Carcinog 34: 113–120.

Wang G, Gastman B, Wieckowski E, Goldstein L, Rabinovitz A, Yin X, Rabinowich H (2001) Apoptosis-resistant mitochondria in T cells selected for resistance to Fas signaling. J Biol Chem 276: 3610–3619.

Yang GH, Jarvis BB, Chung YJ, Pestka JJ (2000) Apoptosis induction by the satratoxins and other trichothecene mycotoxins: relationship to ERK, p38 MAPK, and SAPK/JNK activation. Toxicol Appl Pharmacol 164: 149–160.

Zhou HR, Harkema JR, Hotchkiss JA, Yan D, Roth RA, Pestka JJ (2000) Lipopolysaccharide and the trichothecene vomitoxin (deoxynivalenol) synergistically induce apoptosis in murine lymphoid organs. Toxicol Sci 53: 253–263.

Zhu JS, Halpern GM, Jones K (1998) The scientific rediscovery of an ancient Chinese herbal medicine: *Cordyceps sinensis* Part l. J Altern Complement Med 4: 289–303.

Zhu JS, Halpern GM, Jones K (1998) The scientific rediscovery of a precious ancient Chinese herbal regimen: *Cordyceps sinensis* Part ll. J Altern Complement Med 4: 429–457.